

BEARING CAPACITY OF REINFORCED
CONCRETE THIN-WALL PANELS

©

ELIE EL-CHAKIEH

A Thesis
in
The Department
of
Civil Engineering

Presented in partial fulfillment of the requirement
for the Degree of Master of Engineering at
Concordia University
Montreal, Quebec, Canada

April 1981

© ELIE EL-CHAKIEH, 1981

ABSTRACT

ABSTRACT

BEARING CAPACITY OF REINFORCED
CONCRETE THIN-WALL PANELS

Elie El-Chakieh

Full-scale tests were conducted on pre-fabricated reinforced thin-wall ribbed panels in order to study their overall behavior and determine their Bearing Capacity under in-plane loading.

The cracks appearing on the panels were observed, and deflections were recorded under incremental loading until failure. Recorded ultimate Bearing Capacity loads were compared to those calculated according to The Empirical Method of ACI Building Code, Chapter 14, for wall design (ACI 318-77). The buckling strength of these panels was checked and proved to be not critical.

ACKNOWLEDGEMENTS

ACKNOWLEDGEMENTS

The research reported here was supported by research grants from Natural Sciences and Engineering Council of Canada, Grant No. A1017, Le Program de Formation de Chercheurs et d'Action Concertee, Grant No. FQ- 1645 (Gouvernement du Quebec), and Concordia University.

Spécial gartitude is extended to Dr. Z.A.Zielinski and Dr. M.S. Troitsky for their guidance and advice during the research program.

A word of thanks is extended to Concordia University for the use of the Structural Laboratory and to the technicians B. Leroux and L. Stankevicius for their assistance.

TABLE OF CONTENTS

TABLE OF CONTENTS

	<u>PAGE</u>
ABSTRACT.....	i
ACKNOWLEDGEMENTS.....	ii
LIST OF TABLES.....	iv
LIST OF FIGURES.....	v
NOTATIONS.....	vi
I. INTRODUCTION	
II. PANEL DESCRIPTION AND MATERIAL PROPERTIES	
2.1 Description of Panels.....	3
2.2 Material Properties.....	3
III. EXPERIMENTAL PROCEDURE	
3.1 Test Set-up.....	7
3.2 Test Procedure.....	8
IV. PANEL BEHAVIOR UNDER THE LOADING	
V. ANALYSIS OF TESTS RESULTS	
5.1 Failure Loads.....	14
5.2 Deformation of Panels.....	16
5.3 Load-Strain Relationship	17
5.4 Stability of Panel and Membrane Under Applied Load	18
VI. CONCLUSION.....	28
REFERENCES.....	30
APPENDIX A - TEST PANEL PHOTOGRAPHS.....	31

LIST OF TABLES

LIST OF TABLES

<u>NUMBER</u>	<u>TITLE</u>	<u>PAGE</u>
2.1	Concrete Strength of Panels:.....	4
5.1	Failure Loads and Nominal Bearing Capacity by Equation (5.3)	15
5.2	Overall Deformation at Dial Gage Positions	17

LIST OF FIGURES

v

LIST OF FIGURES

<u>FIGURE</u>	<u>DESCRIPTION</u>	<u>PAGE</u>
2.1	Typical Thin-wall Panel - Dimensions and Reinforcement Details.....	5
2.2	Reinforcement Stress-Strain Relationships.....	6
3.1	Experimental Set-Up.....	9
4.1	Experimental Crack Patterns of Panel C1.....	11
4.2	Experimental Crack Patterns of Panel C2.....	12
4.3	Experimental Crack Patterns of Panel C3.....	13
5.1	Horizontal Displacement and Deformation of Nodes C ₃	24
5.2	Overall Displacement and Deformation of Panel C1.....	25
5.3	Overall Displacement and Deformation of Panel C2 and C3.....	26
5.4	Load-Strain Relationship.....	27
5.5	Vertical Rib.....	20
5.6	Membrane Unit Width.....	21

NOTATIONS

NOTATIONS

A	Area of transformed rib cross-section
a	Membrane Plate length
A_g	Gross cross-sectional area
$(A_s)_b$	Area of reinforcing bar in longitudinal ribs
$(A_s)_m$	Area of reinforcing wire in membrane
A_t	Overall transformed cross-sectional area
b	Membrane Plate width
D, D_t	Flexural rigidity of membrane plate and its transformed section, respectively
E_c, E_s	Modulus of elasticity of concrete and steel, respectively
F	Test failure load
f'_c	Compressive strength of concrete
f_y	Yield strength of reinforcement
h	Overall thickness of the wall panel
I_t	Moment of inertia of transformed rib cross-section
$(I_t)_m$	Moment of inertia of transformed unit length of membrane section
l_c	Overall length of wall panel
m'	Number of half wave lengths
m	Yield strength ratio of steel to concrete
n	Modulus of elasticity ratio of steel to concrete
P	Applied load
P_u	Ultimate bearing capacity
\bar{P}_u	Nominal bearing capacity
t	Thickness of membrane plate
W	Normal weight of concrete
w	Overall width of wall panel
ϵ	Limit compressive strain in concrete
θ	Term defined by equation (5.5)
ν	Poisson's ratio for concrete
ρ_m	Ratio of yielded steel to gross area

ρ_n	Ratio of non-yielded steel to gross area
σ_{cr}	Critical buckling strength
ϕ, ψ	Terms defined by equation (5.5)
ϕ	Capacity reduction factor

CHAPTER I

INTRODUCTION

CHAPTER I
INTRODUCTION

Prefabricated thin-wall concrete panel systems are presently widely used in building industry. For example, such panels have been used on numerous projects for walls and floors in low-cost housing by Zielinski (1), (2).

Strength and behavior of thin-wall ribbed panels became a subject of ongoing research work at Concordia University. Earlier research included ribbed panels working as wall-beam elements (3). Other research was done on reduced scale walls of constant thickness (4).

Not much research data is available on the strength of ribbed thin-wall panels; this is what prompted the research work here. The main purpose of this research was to study, on full scale models, the Ultimate Bearing Capacity of prefabricated thin-wall panels, of symmetrical cross-section, and to verify the applicability of the design method presently recommended for walls by the ACI Building Code of Practice for Reinforced Concrete (ACI 318-77) (5). Analysis of such panels led to the determination of equations which were applicable to the design of walls.

A parallel research, to the one presented in this report, at Concordia University, included testing of thin-wall panels of unsymmetrical cross-section for the determina-

tion of their Bearing Capacity and strength evaluation according to ACI recommendation for design of walls (6).

CHAPTER II

PANEL DESCRIPTION AND MATERIAL PROPERTIES

CHAPTER II

PANEL DESCRIPTION AND MATERIAL PROPERTIES

2.1 DESCRIPTION OF PANELS

The panels were produced in 1975. Some of the panels then produced were used in earlier research as wall beams. The panels had overall dimensions of 89" x 44", and were made of thin-wall slab membrane only $1\frac{1}{2}$ " thick, with 3" x 6" ribs all around the perimeter, thus forming a thin-walled symmetrical structural element of I-cross section. These ribs were provided in order to accommodate the perimeter reinforcing bars and to increase the overall rigidity, as it was required for walls in buildings.

All panels contained a 6 X 6 - 6/6 welded wire fabric mesh as wall membrane reinforcement and 2 # 4 Bars as rib main reinforcement. Dimensions of panels and reinforcement details are shown in Fig. 2-1.

2.2 MATERIAL PROPERTIES

The strength of concrete used for panels was tested by Taner (3) in 1975 on 6" dia. cylinders at 90 days age. It was assumed, based on the Code of Practice of Reinforced Concrete by the European Concrete Committee (7), that the strength of concrete at time of testing panels, in September 1980, increased by approximately 12.5%. Both 90 days- and present-test strengths of concrete are given in table 2.1.

TABLE 2-1 CONCRETE STRENGTH OF PANELS

Panel No.	Strength at 90 days f'_c , PSI	Estimated Strength at Testing f'_c , PSI
C1	5382	6055
C2	5382	6055
C3	6446	7252

The strength of steel reinforcement was $f_y = 60.1$ ksi for #3 bars and $f_y = 78.4$ ksi for welded wire fabric mesh. The stress-strain diagram for steel reinforcement is shown in Fig.2-2.

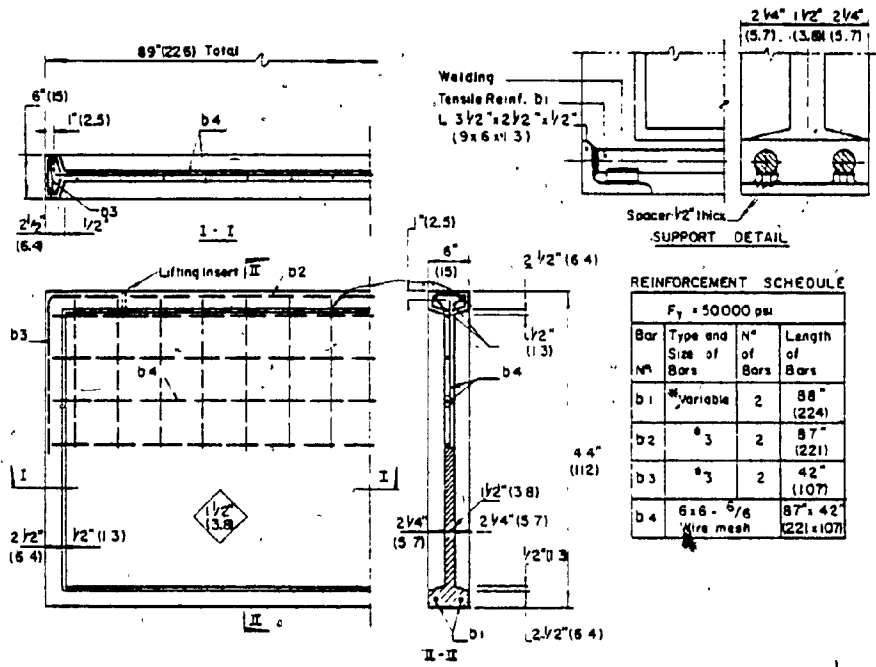


Fig. 2.1 Typical Thin-Wall Panel - Dimensions and Reinforcement Details

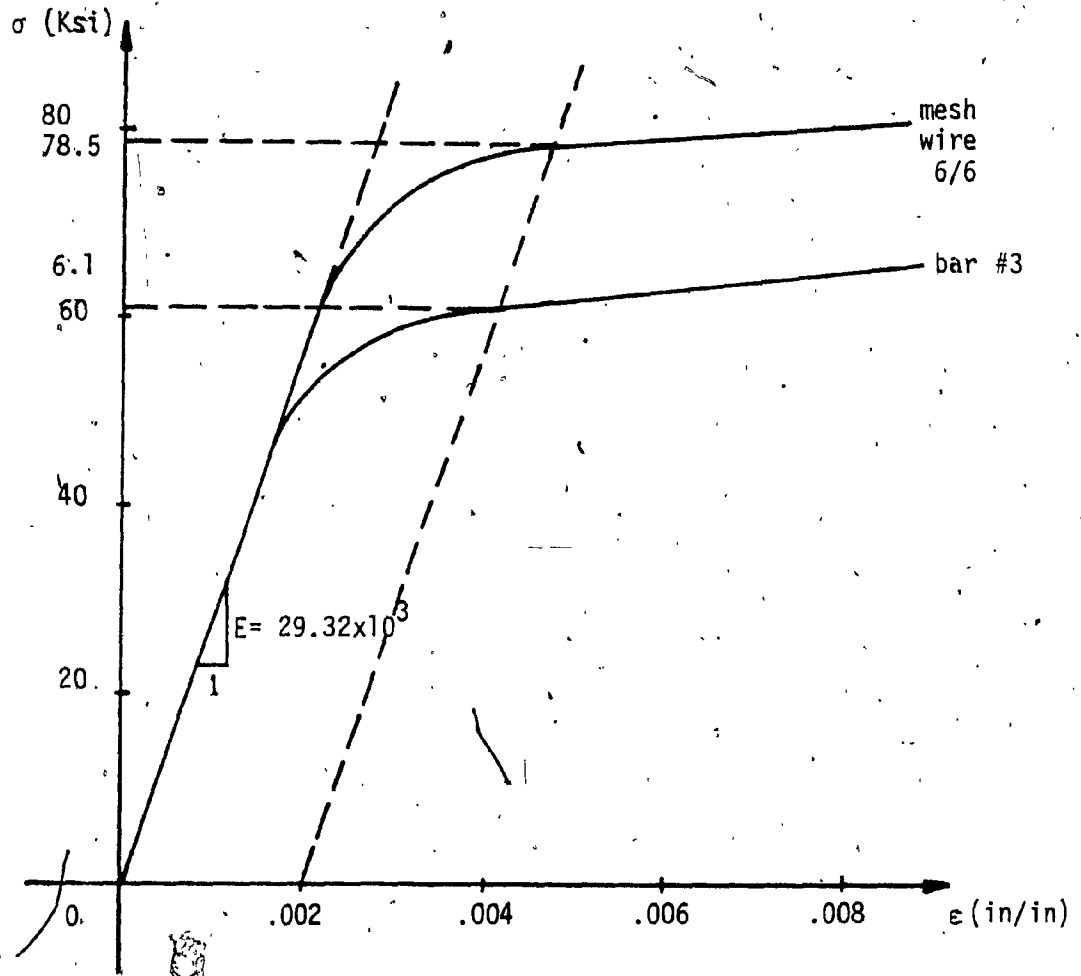


Fig. 2.2 Reinforcement Stress-Strain Relationship.

CHAPTER III.

EXPERIMENTAL PROCEDURE

CHAPTER III

EXPERIMENTAL PROCEDURE

3.1 TEST SET-UP

The panels were tested in the vertical position in a steel frame as shown in Fig. 3-1. The loading set-up consisted of an overhead mounted hydraulic jack with loading cell and strain indicator, which were calibrated prior to testing. The panels were cleaned and painted white before testing. A line grid was drawn on each of the panels to facilitate observation and location of cracks. Some shrinkage (or handling) cracks existed on all panels which were marked in orange color on panels and reproduced with dotted lines in Figs. 4-1 to 4-3. The panels were placed in the testing frame with 6" X 44" X $\frac{1}{4}$ " masonite boards as bearing pads on top and bottom. Additionally, fresh mortar of approximately $\frac{1}{4}$ " was placed between the panel's surface and masonite board, in order to obtain a uniform load transfer. A rigid steel beam was then placed at the top, under the loading jack and loading cell. Dial gages were used to measure panel displacements. These were placed at every intersection of grid lines enabling the plane deformation of the membrane and of the entire structure to be recorded Fig. 3-1. Additional dial gages were used to determine the panel's shortening along its centerline.

3.2 TEST PROCEDURE

The panels were tested as wall bearing elements. The loading was done incrementally. The initial load applied was 46 kips, followed by increments of 23 kips. Cracks were observed and marked on the panels as they occurred at every load increment; and were given a number besides, indicating the load magnitude at which they occurred.

Loading was done in two stages. In the first stage, panels were loaded up to about one-half of the predicted failure load, and released afterwards. In the second stage, the panels were loaded from zero load up to failure. A minimum of six hours time was given between the two stages for panel's stress release and measurement of remaining plastic deformation.

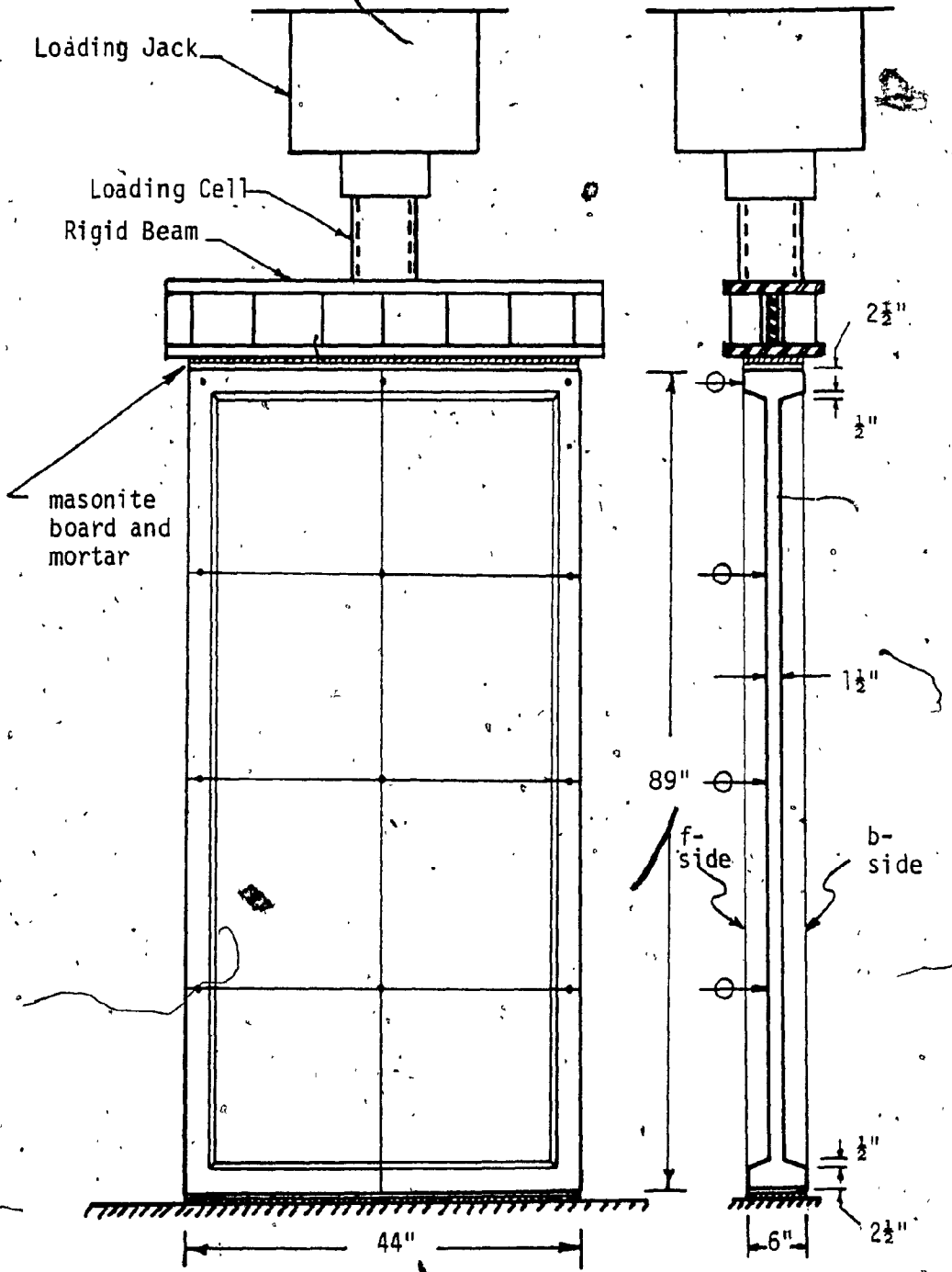


FIG. 3-1

EXPERIMENTAL SET-UP

CHAPTER IV

PANEL BEHAVIOR UNDER THE LOADING

CHAPTER IV

PANEL BEHAVIOR UNDER THE LOADING

In general, two types of cracks horizontal and vertical occurred during the loading. The occurrence of cracks was sequential. Horizontal cracks occurred on the vertical ribs between loads of 46-114 kips, and were followed by vertical cracks on the wall membrane. The vertical cracks were predominant in all panels. They were observed first on horizontal top and bottom ribs, and on rib faces away from the bearing surface, at loads from 92 kips to 229 kips, and in the wall membrane at 69 kips upto failure. The vertical cracks in the membrane usually occurred suddenly, audibly and over an extensive length.

The existing shrinkage (or handling) cracks did not influence significantly the propagation of new cracks under loading. It was also observed that existing horizontal shrinkage cracks closed under increasing loading.

Failure normally occurred suddenly along the horizontal or slightly inclined lines close to the junction of the wall membrane with the horizontal ribs. Failure cracks in the final stage propagated along vertical ribs separating them from the slab membrane. The cracking patterns and failure modes for all panels are illustrated in Figs. 4-1, 4-2 and 4-3.

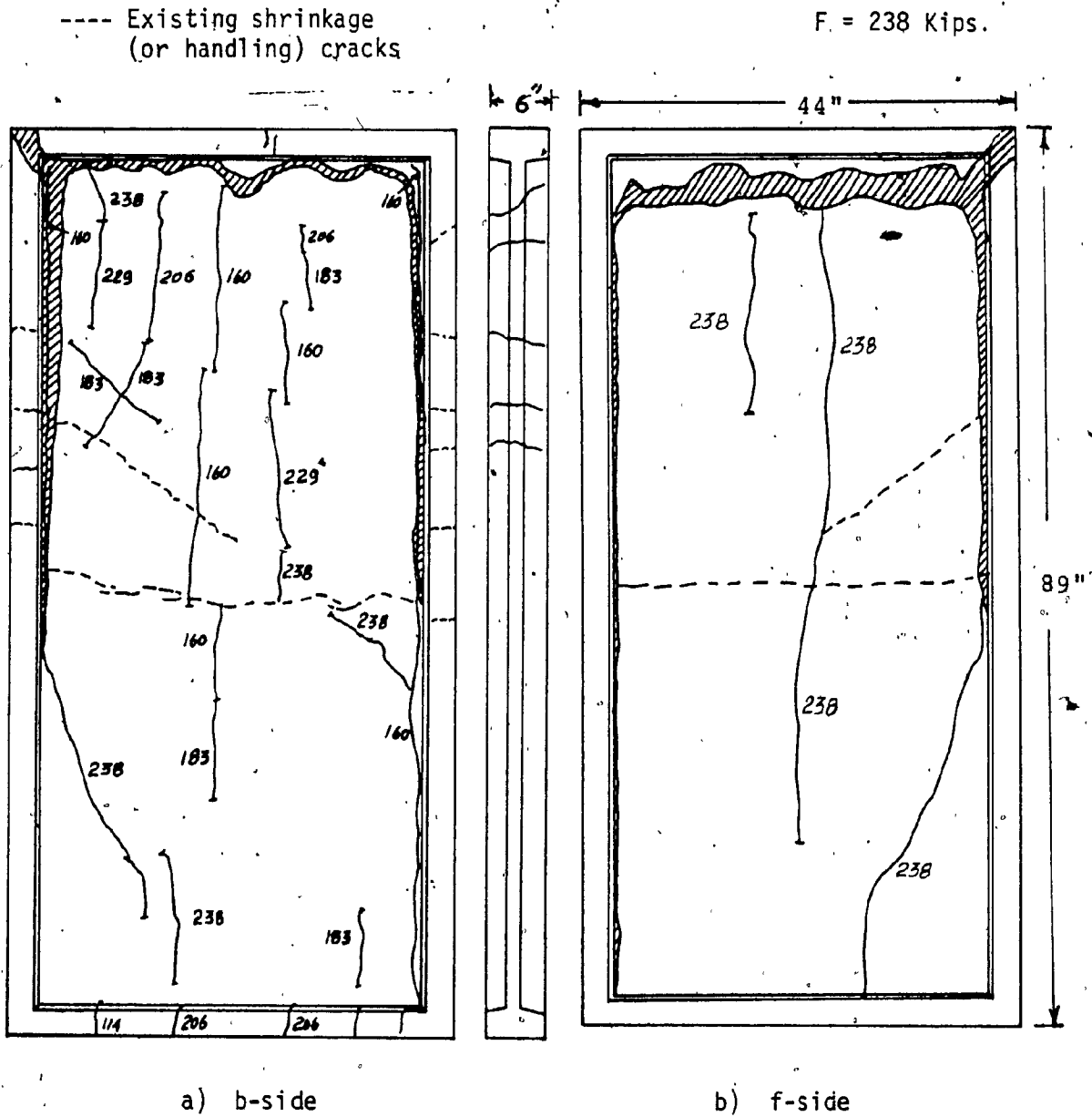
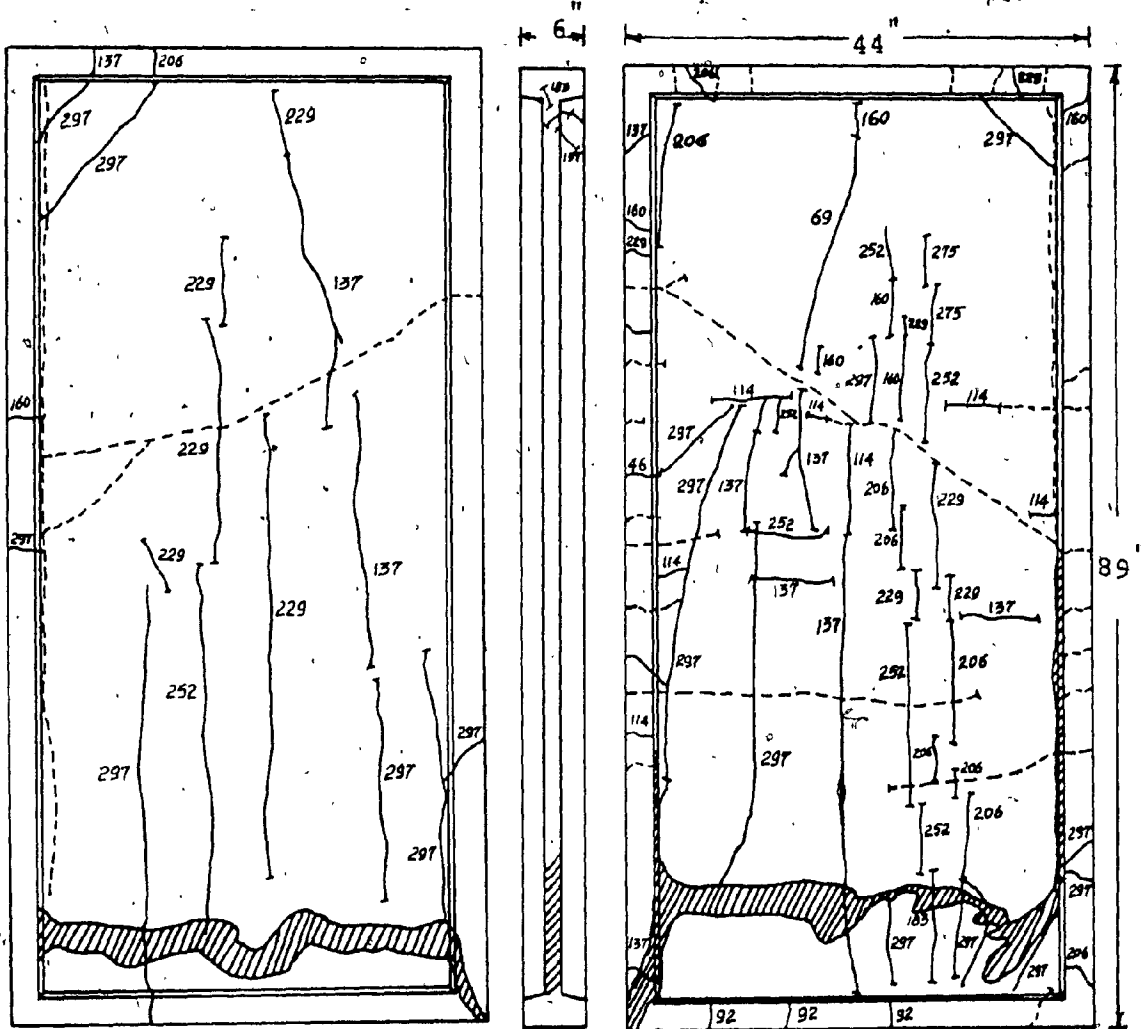


Fig. 4.1 EXPERIMENTAL CRACK PATTERNS OF PANEL C1.

---- Existing shrinkage
(or handling) cracks

F = 297 Kips.



a) b-side

b) f-side

Fig. 4-2 EXPERIMENTAL CRACK PATTERNS OF PANEL C2

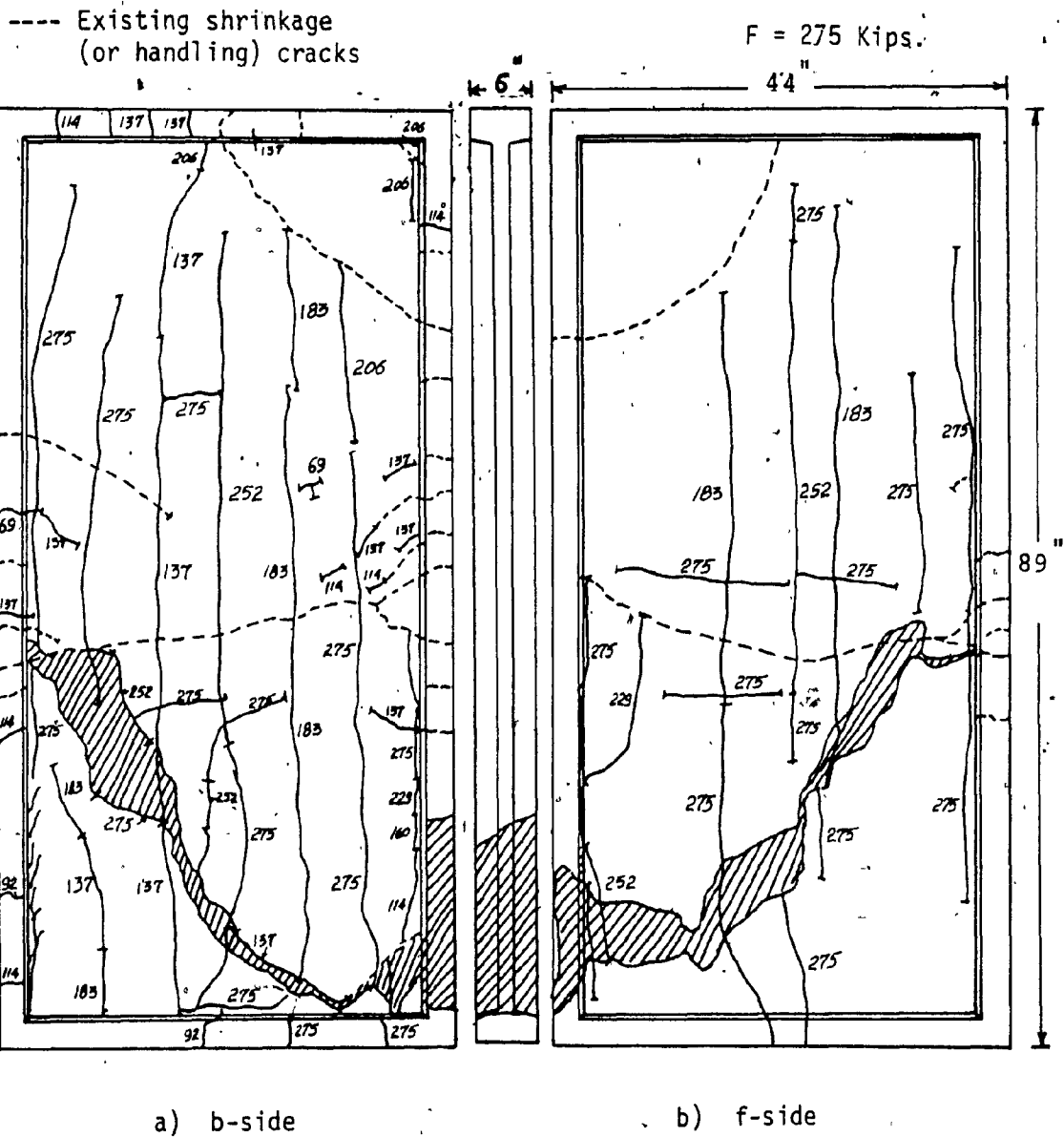


Fig. 4-3 EXPERIMENTAL CRACK PATTERNS OF PANEL C3.

CHAPTER V

ANALYSIS OF TEST RESULTS

CHAPTER V

ANALYSIS OF TEST RESULTS

5.1 FAILURE LOADS.

Failure loads can be calculated according to the ACI Building Code (ACI 318-77) (6). Equation 14.1 of Chapter 14 gives the Ultimate Bearing Capacity of a wall, under axial loading, as

$$P_u = 0.55 \phi f'_c A_g \left[1 - \left(\frac{l_c}{40h} \right)^2 \right] \quad (5.1)$$

The above equation should be modified if it is to take into account the presence of steel reinforcement as follows :

$$P_u = 0.55 \phi f'_c A_g \left[1 - \left(\frac{l_c}{40h} \right)^2 \right] \cdot [1 + (n-1)\rho_n + (m-1)\rho_m] \quad (5.2)$$

Considering the nominal bearing capacity as

$$\bar{P}_u = \frac{P_u}{\phi}, \text{ equation (5.2) can be rewritten as}$$

$$\bar{P}_u = 0.55 f'_c A_g \left[1 - \left(\frac{l_c}{40h} \right)^2 \right] [1 + (n-1)\rho_n + (m-1)\rho_m] \quad (5.3)$$

For panel C1 with $f'_c = 6055$ psi, the nominal failure load \bar{P}_u can be calculated using equation (5.3)

as follows :

$$\bar{P}_u = 0.55 \times 6.055 \times 90.75 \left[1 - \left(\frac{89}{40 \times 6} \right)^2 \right] \left[1 + (6.54 - 1) \frac{0.203}{90.75} + \left(\frac{60.1}{6.055} - 1 \right) \times \frac{0.44}{90.75} \right] = 275 \text{ Kips.}$$

The corresponding failure load recorded during test was

$$F = 238 \text{ kips.} = 0.865 \bar{P}_u$$

A comparison of failure loads so calculated, with test results are shown in table 5.1 for all panels tested.

TABLE 5.1 FAILURE LOADS AND NOMINAL BEARING CAPACITY By EQⁿ
(5.3)

Panel No.	Concrete Strength f'_c , psi	Test failure Load F, kips.	Nominal Bearing Capacity \bar{P}_u Kips.	Capacity Reduction Factor $\phi = \frac{F}{\bar{P}_u}$
C1	6055	238	275	0.865
C2	6055	297	275	1.079
C3	7252	275	327	0.842
Average	6454	270	292	0.929

5.2 DEFORMATION OF PANELS

All panels showed a similar mode of deflection. The horizontal displacement and deformation of center point of panels C2 and C3 (nodes C_3) are illustrated in Fig. 5.1.

As deformation, we call the measured relocation from original position, and as displacement - the net value of deformation. As it can be seen from Fig. 5.1, the maximum displacement recorded for center points (C_3) was in the range of 0.003" to 0.00375". A very small plastic deformation after reloading (≈ 0.0002 ") was recorded. Overall deformation patterns indicate that there was no loss of stability of the membrane wall. Overall displacement and deformation curves of the panels are shown in Figs. 5.2 and 5.3, and table 5.2 illustrates the overall deformation at dial gage positions.

TABLE 5.2 OVERALL DEFORMATION AT DIAL GAGE POSITIONS

Dial Gage Position	Panel No.	Deformation (in $\times 10^{-3}$)		
		C1	C2	C3
Left Side	L1	+10	-81	-52
	L2	-154	-75	+14
	L3	-6	0	+24
	L4	-53	+4	-9
Center Line	C1	-44	-11	-9
	C2	-228	-1	+57
	C3	-143	+20	+7
	C4	-169	+25	-99
Right Side	R1	-97	-88	-17
	R2	-178	-16	+3
	R3	-78	+18	-32
	R4	-4	+22	-51

5.3 LOAD STRAIN RELATIONSHIP

The load strain relationship of panel centerlines are illustrated in Fig. 5.4. Curves (I) and (II) are for first and second stages of loading respectively. It is noticed from the above diagrams that panels showed elastic behavior in the initial stage of loading (Curve I) up to 137 kips. This elastic behavior was also continued in the second stage of loading up to about 252 kips (85%-90% of failure load values) and then strain increased suddenly. The strain values recorded at failure were between 0.00225 to 0.0026 in/in which are in relatively good agreement with

ACI limit strain value ($\epsilon = 0.003$).

5.4 STABILITY OF PANEL AND MEMBRANE UNDER APPLIED LOAD

The overall stiffening effects of the panel was provided by perimeter ribs. It can be assumed that vertical ribs act as lateral elastic supports to the membrane, thus the membrane deforms from wall plane together with the ribs. No displacement can occur at the top and bottom because of the horizontal ribs and friction between ribs and bearing surface. Overall stiffness of the system of membrane and perimeter ribs should be considered while evaluating the critical buckling strength of the panel.

Under the applied load both vertical ribs can deflect in the same direction or in opposite directions. According to Timoshenko (8), if side ribs were assumed to deflect in opposite directions, a transcendental equation would be obtained which would lead to critical strength values higher than when ribs deflect in the same direction. Thus it is advisable to analyse first the system where both ribs deflect in same direction. If such a model shows that the critical load is greater than the static carrying capacity of panel, this means that buckling is not the critical phenomenon and it would not be necessary to check the transcendental equation. In the following analysis, torsional rigidity is neglected because of symmetry of

cross-section in both directions, and because the panel is pin supported at top and bottom which leads to lower critical strength values.

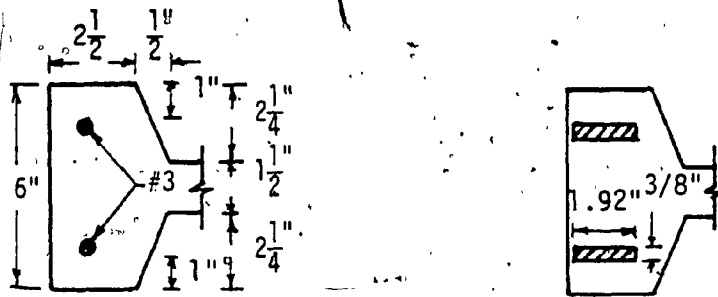
The critical buckling strength of a plate stiffened with longitudinal edge ribs (parallel to direction of loading), and simply supported along top and bottom end edges (perpendicular to direction of applied load), can be defined following Timoshenko (8) by Caliřev's equation as,

$$\sqrt{\psi-\phi} [\psi+(1-\nu)\phi]^2 \tan \frac{1}{2} \sqrt{\psi\phi+\phi^2} + \sqrt{\psi+\phi} [\psi-(1-\nu)\phi]^2 \tanh \frac{1}{2} \sqrt{\psi\phi-\phi^2} = 2\phi^{5/2} \psi\theta \quad (5.4)$$

Where

$$\left. \begin{aligned} \phi &= m' \pi \frac{b}{a} \\ \psi &= b \sqrt{t \frac{\sigma_{cr}}{D_t}} \\ \theta &= \frac{E_c I_t}{b D_t} - \frac{A}{b t} \frac{\psi^2}{\phi^2} \\ \nu &= \text{Poisson's ration} = \frac{1}{6} \end{aligned} \right\} \quad (5.5)$$

For the calculation of stiffness properties a transformed cross-section is considered recognizing the ratio of modulus of elasticity of steel to concrete. For the vertical ribs the transformed cross section is shown in Fig. 5.5.



a) rib cross-section

b) rib transformed cross-section

Fig. 5.5 Vertical Rib

The modulus of elasticity of steel is

$$E_s = 29.32 \times 10^3 \text{ (from fig. 2.2)}$$

The modulus of elasticity of concrete according to (ACI-318-77) (6) is

$$E_c = 33 (w)^{1.5} \sqrt{f'_c} \quad (5.6)$$

For panel C1,

$$E_c = 4.484 \times 10^3 \text{ ksi}$$

$$n = \frac{E_s}{E_c} = 6.54$$

$$(A_s)_b = 0.11 \text{ in}^2 \text{ per each reinforcing bar}$$

$$n(A_s)_b = 6.54 \times 0.11 = 0.72 \text{ in}^2$$

Width of transformed section of each steel bar

$$= \frac{0.72}{0.375} = 1.92 \text{ inches}$$

The moment of Inertia of the transformed section is

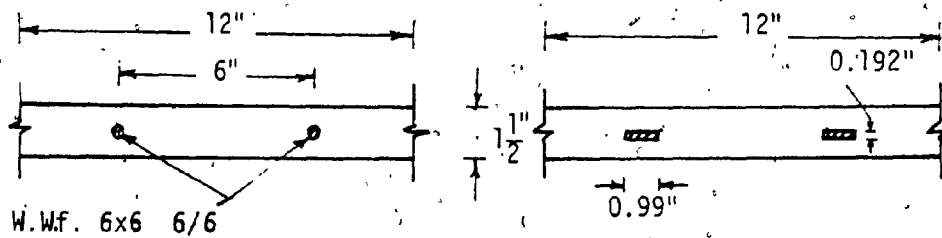
$$I_t = 52.0 \text{ in}^4$$

The flexural rigidity of the membrane plate per unit

$$\text{width is } D = \frac{E X t^3}{12 (1-\nu^2)} \quad (5.7)$$

The flexural rigidity of the transformed membrane section is

$$D_t = \frac{E_c X (I_t)_m}{(1-\nu^2)} \quad (5.8)$$



a) Membrane Cross-section

b) Membrane transformed cross-section

Fig. 5.6 Membrane Unit Width

$$(A_s)_m = 0.058 \text{ in}^2/\text{ft.}$$

$$n(A_s)_m = 6.54 \times 0.058 = 0.38 \text{ in}^2/\text{ft.}$$

Width of transformed section of each mesh wire

$$= \frac{0.38}{2} = 0.99"$$

The moment of Inertia of transformed section of the membrane having 1" width = $(I_t)_m = \frac{3.376}{12}$ in⁴. equation (5.8) then gives

$$D_t = \frac{1}{12} \frac{E_c \times 3.376}{[1 - (\frac{1}{6})^2]} = 0.28940 E_c = 1297.5415 \text{ K-in}^2$$

The term $\frac{E_c I_t}{b D_t} = \frac{E_c \times 52}{38 \times 0.28940 E_c} = 4.72887$

and $\frac{A}{b t} = \frac{2[(2.5+3) \times 2.25/2 - 0.11 + 0.72] + 3 \times 1.5}{38 \times 1.5} = \frac{18.095}{57}$
 $= 0.31746$

From equation (5.5) : The following is obtained :

$$\phi = 1 \times \pi \times \frac{38}{83} = 1.43832$$

$$\psi = 38 \frac{\sqrt{1.5 \sigma_{cr}}}{1297.5415} = 1.29202 \sqrt{\sigma_{cr}}$$

$$\theta = 4.72887 - 0.25616 \sigma_{cr}$$

where σ_{cr} is the critical stress in (Ksi).

By substituting the above values in equation (5.4) The following is obtained;

$$\begin{aligned} & \left[\left(\sqrt{1.29202 \sqrt{\sigma_{cr}} - 1.43832} \right) \left[1.29202 \sqrt{\sigma_{cr}} + \left(1 - \frac{1}{6}\right) (1.43832) \right]^2 \right. \\ & \left. \times \left[\tan \frac{1}{2} \sqrt{1.29202 \sqrt{\sigma_{cr}} (1.43832) - (1.43832)^2} \right] + \right. \\ & \left. + \left[\sqrt{1.29202 \sqrt{\sigma_{cr}} + 1.43832} \right] \left[1.29202 \sqrt{\sigma_{cr}} - \left(1 - \frac{1}{6}\right) (1.43832) \right]^2 \right. \\ & \left. \times \left[\tanh \frac{1}{2} \sqrt{1.29202 \sqrt{\sigma_{cr}} (1.43832) + (1.43832)^2} \right] \right] \\ & = \left\{ 2(1.43832) \times 1.29202 \sqrt{\sigma_{cr}} (4.72887 - 0.25616 \sigma_{cr}) \right\} \end{aligned}$$

By trial and error method, the solution to the above equation yields ;

$$\sigma_{cr} = 7.515 \text{ Ksi}$$

The transformed cross-sectional area of the panel

$$\begin{aligned} A_t &= 2(18.095) + (38 \times 1.5) - 7(0.029) + 7(0.38/2) \\ &= 94.32 \text{ in}^2 \end{aligned}$$

Hence the critical load for buckling failure of the panel is:

$$P_{cr} = \sigma_{cr} \times A_t = 7.515 \times 94.32 = 708.8 \text{ kips.}$$

The above critical buckling load is much higher than the failure load recorded. Hence there is no need to consider the transcendental equation in evaluating the critical buckling strength of the panel, nor to go into a more exact analysis recognizing influence of other contributing parameters mentioned earlier. For panel C2, the critical buckling stress would be the same as for panel C1. However, the critical stress for panel C3 is higher because of higher concrete compressive strength.

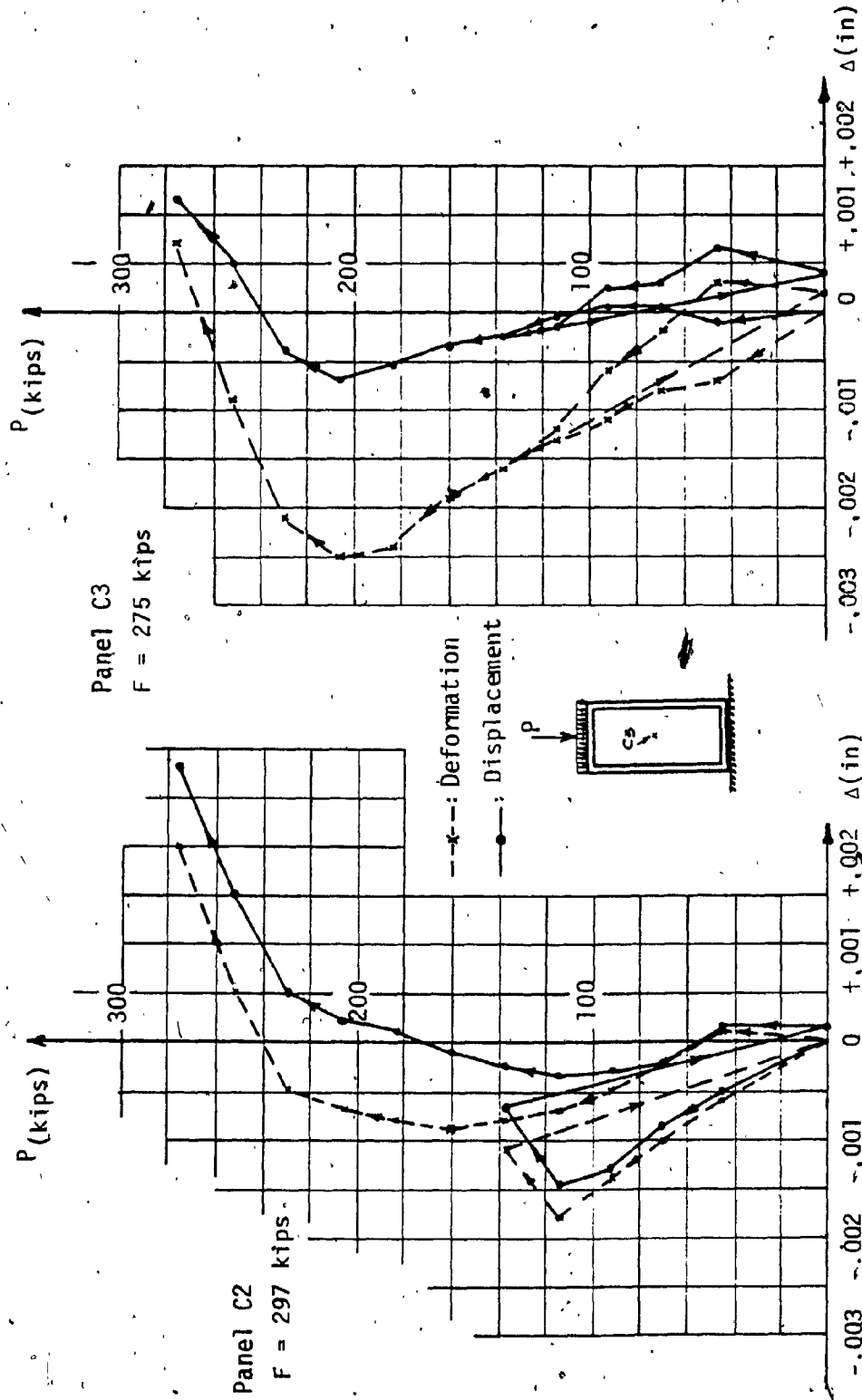


Fig. 5.1 HORIZONTAL DISPLACEMENT & DEFORMATION OF NODES-C₃

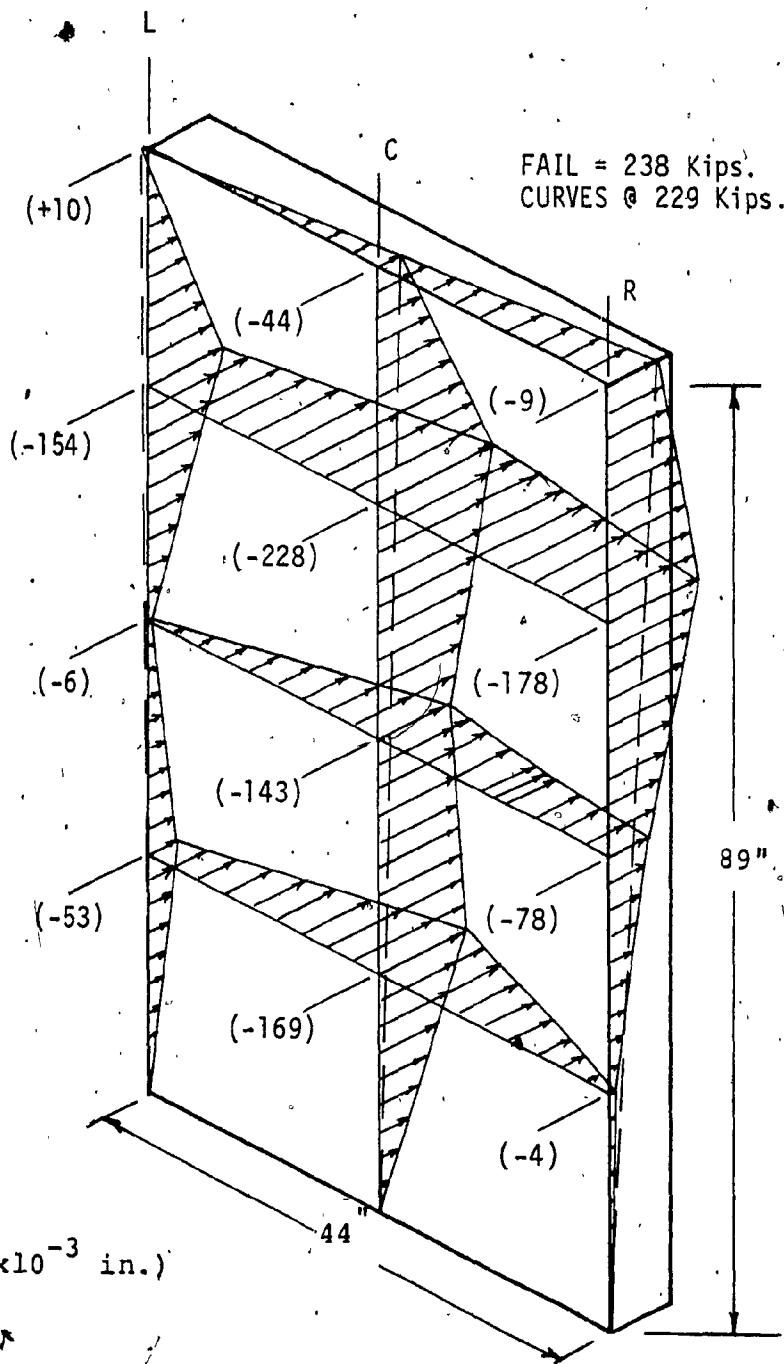


Fig. 5.2 OVERALL DISPLACEMENT AND DEFORMATION OF PANEL C1

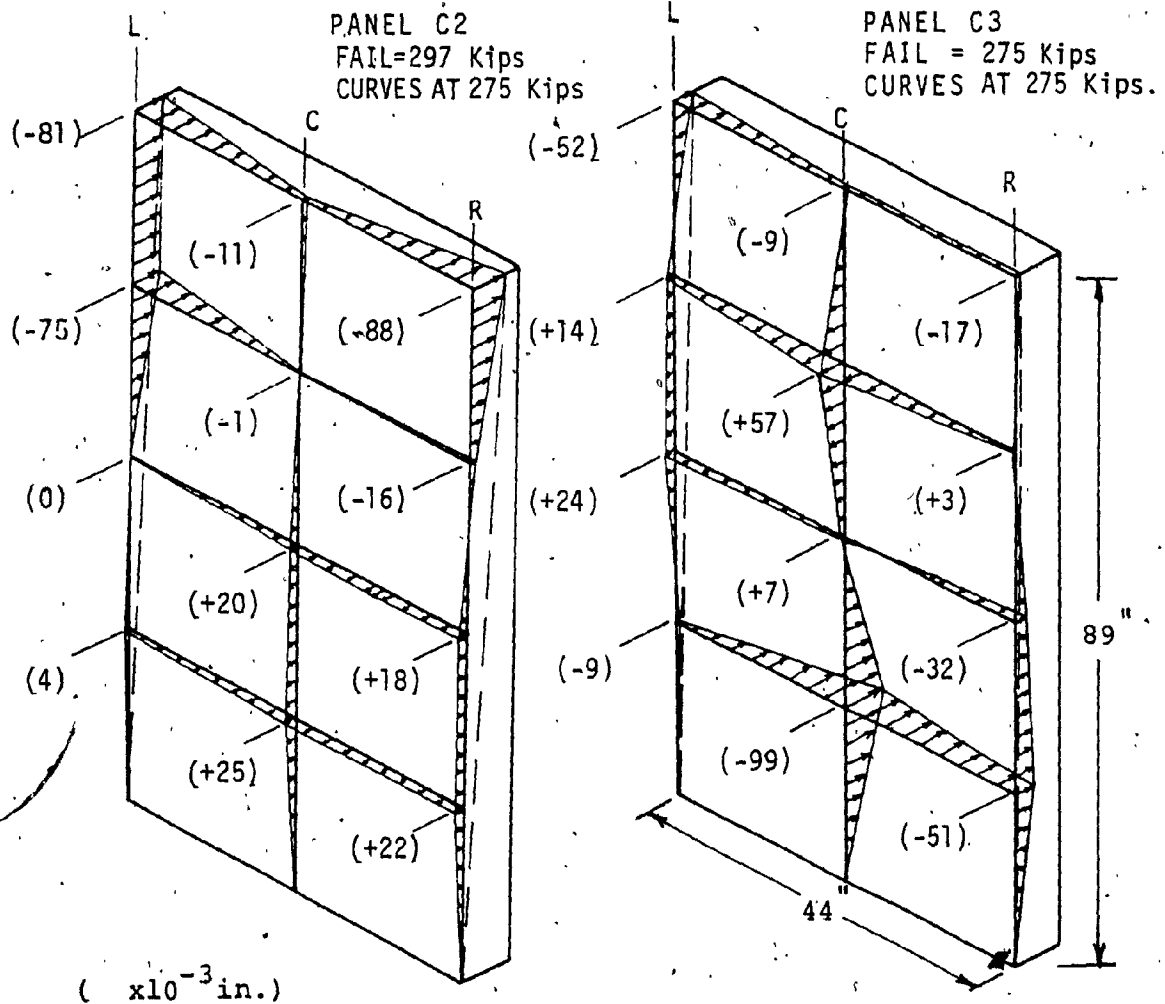


Fig. 5.3 OVERALL DISPLACEMENT AND DEFORMATION OF PANELS C2 AND C3.

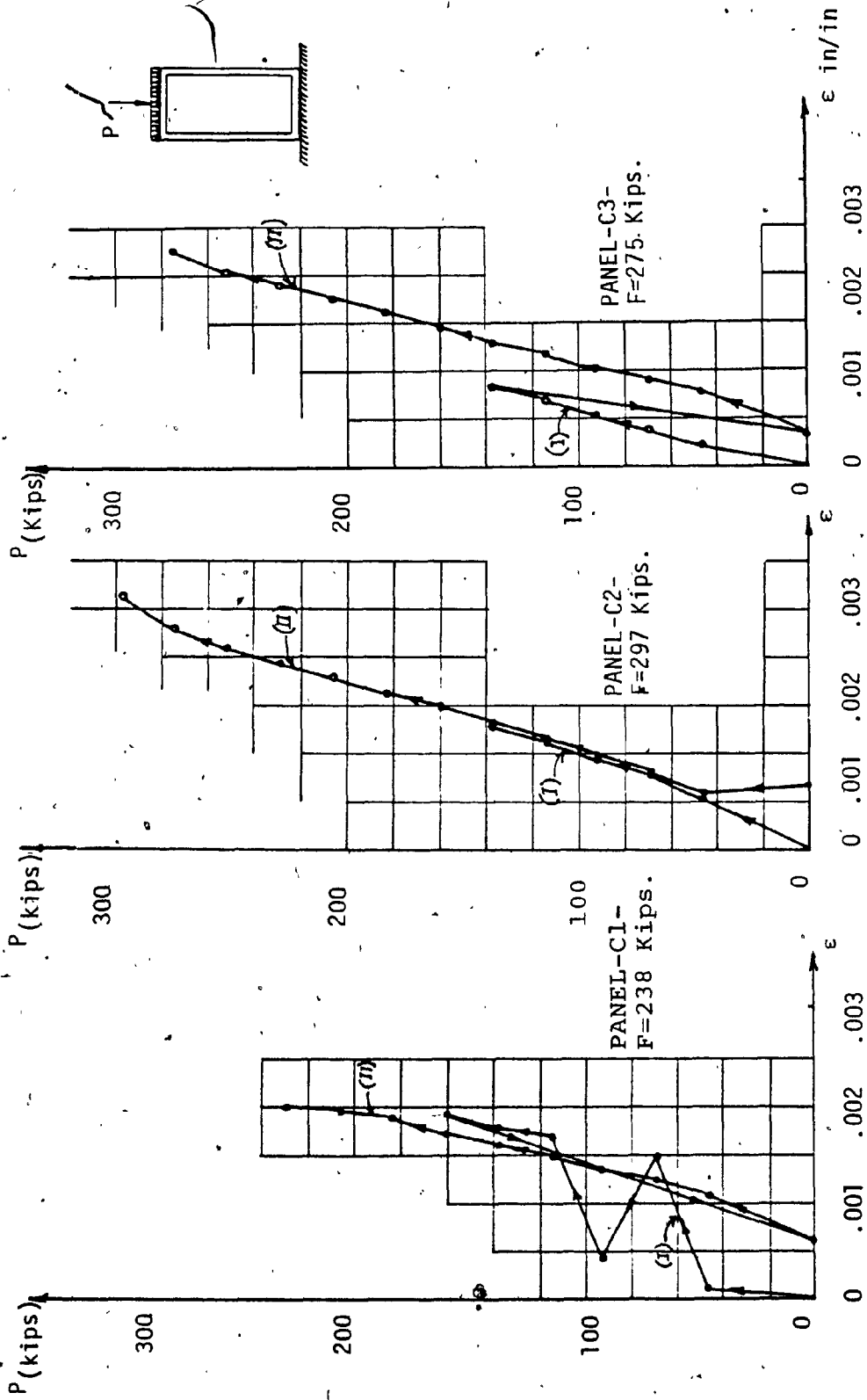


Fig. 5.4 Load-Strain Relationship.

CONCLUSION

Test results and analysis of thin-wall panels discussed in this report lead to the following conclusions.

1. Panels tested showed higher strengths than the predicted values according to the present ACI practice for wall design (ACI 318-77). However the validity of this conclusion should not be generalized until more tests are carried out.
2. Strength of panels was not influenced by overall stiffness and buckling phenomena: such panels having the following dimensional relationships: $\frac{l_c}{h} \leq 15$; $\frac{w}{t} \leq 30$; $\frac{h}{t} \leq 4$. Buckling was evaluated according to Timoshenko and showed values higher than failure loads recorded.
3. Under load, panels showed different modes of deformations. In some panels the ribs and membrane deflected in the same direction and the others showed deflections in opposite directions. The maximum recorded deformation was $\frac{1}{390} \times l_c$. Membrane plate showed almost no loss of stability under loading (≈ 0.00375 ").
4. No significant discrepancy was recorded with load-strain relation under loading. Measured strain carried almost up to failure time was approximately 0.0026 in/in which

is less than limit strain of 0.003 used by ACI for ultimate design of flexural members. Panels behaved elastically up to 85% of failure load values and then the strain increased suddenly.

5. All panels showed almost the same cracking pattern under load. Vertical cracks along compression direction started to occur at loads close to 137 kips.
6. Failure of panels in all cases occurred near the junction along the same line perpendicular to load direction. The failure cracks of panels propagated along vertical ribs separating them from the membrane plate.
7. Further research should be carried out on thin-wall panels having variable dimensions and strength to determine the critical parameters which will induce critical buckling strength.

REFERENCES

1. Zielinski, Z.A., "Building Industrialization Trends in India", Industrialization Forum, Vol. 3, No. 2, Dec. 1971.
2. Zielinska, Cz. and Zielinski, Z.A., "Prefabrication Systems for Low Cost Housing", International Conference on Industrial Building Processes, Proceeding, West Virginia University, 1972.
3. Taner, N., "Strength and Behaviour of Beam-Panels - Tests and Analysis", ACI Journal, vol. 74, No. 48, (October 1977), pp. 511-520.
4. Oberlender, G.D. and Everard, N.J., "Investigation of Reinforced Concrete Walls" , ACI Journal, Vo. 74, No. 28, (June 1977), pp. 256-263.
5. ACI Committee 318, "Building Code Requirements for Reinforced Concrete (ACI 318-77)", American Concrete Institute, Detroit, 1977.
6. Troitsky, M.S., Zielinski, Z.A. and Christodoulou, H., "Investigation of Bearing Capacity on Thin Wall Ribbed Reinforced Concrete Panels," Eight Canadian Congress of Applied Mechanics, Proceedings, Moncton University, 1981.
7. American Concrete Institute., Cement and Cement and Concrete Association., "Recommendations for an International Code of Practice for Reinforced Concrete".
8. Timoshenko, and Gere., "Theory of Elastic Stability", McGraw-Hill Book Co., 2nd Edition, 1961.

APPENDIX A

TEST PANEL PHOTOGRAPHS

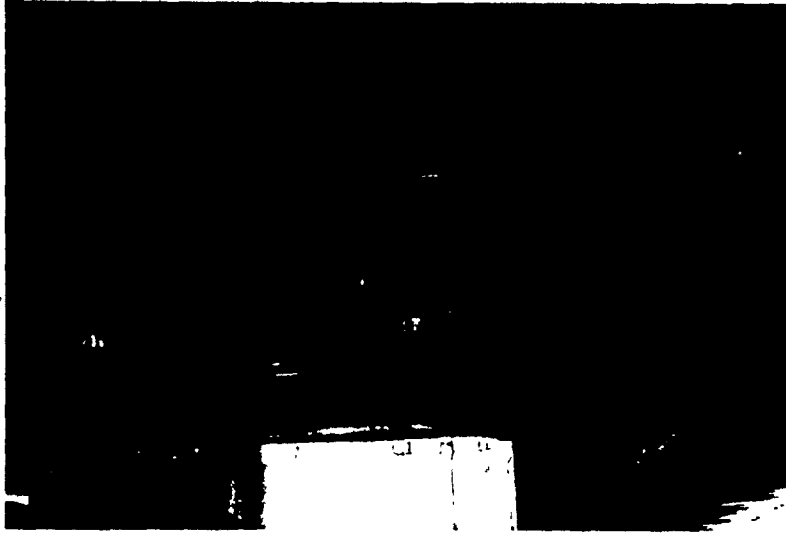


Figure A1
Loading Arrangement



Figure A2
Panel In Testing Frame

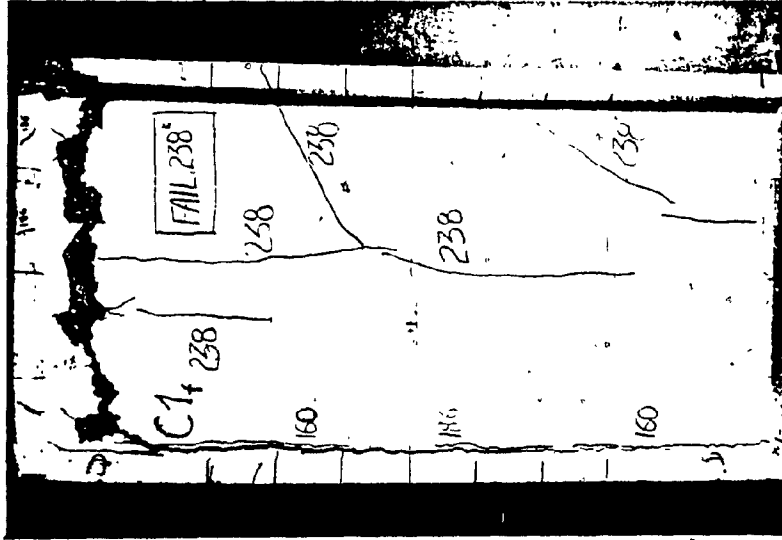


Figure A4
Front View of Panel C1 (At Failure)

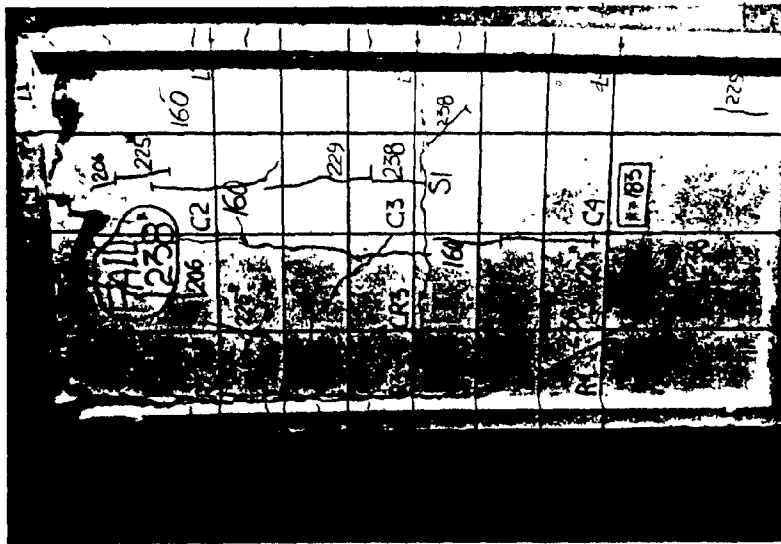


Figure A3
Back View of Panel C1 (At Failure)

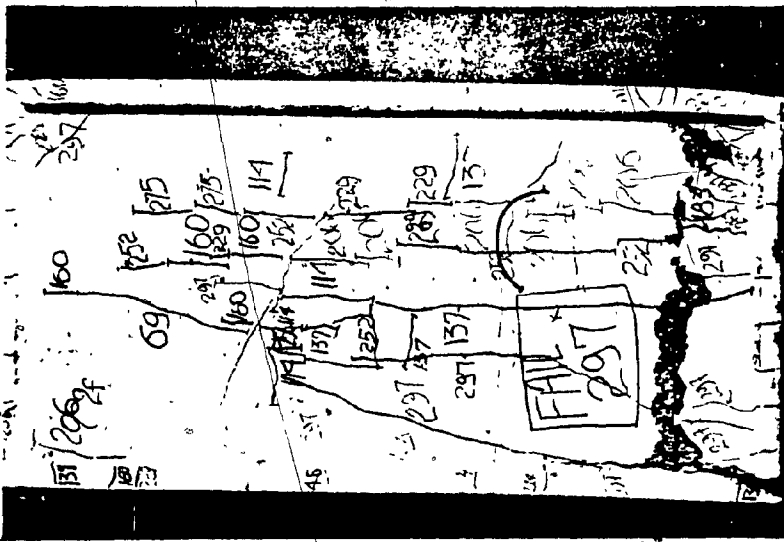


Figure A6
Front View of Panel C2 (At Failure)

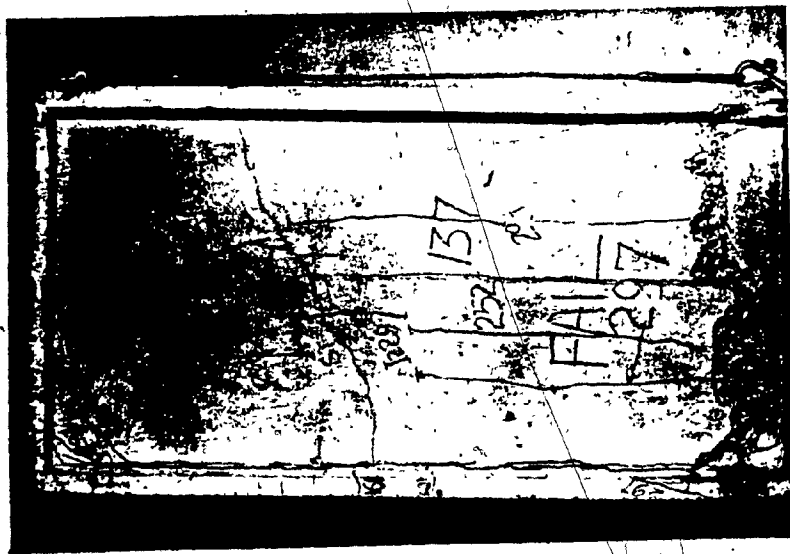


Figure A5
Back View of Panel C2 (At Failure)

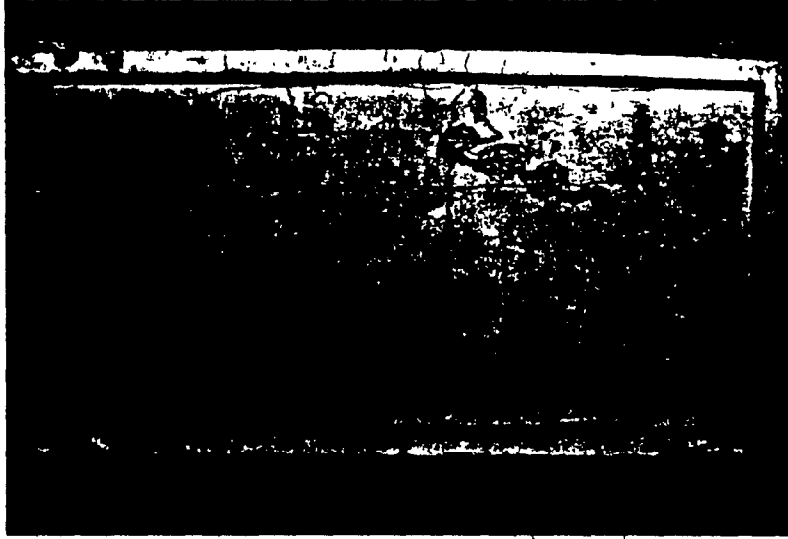


Figure A8
Front View of Panel C3 (At Failure)

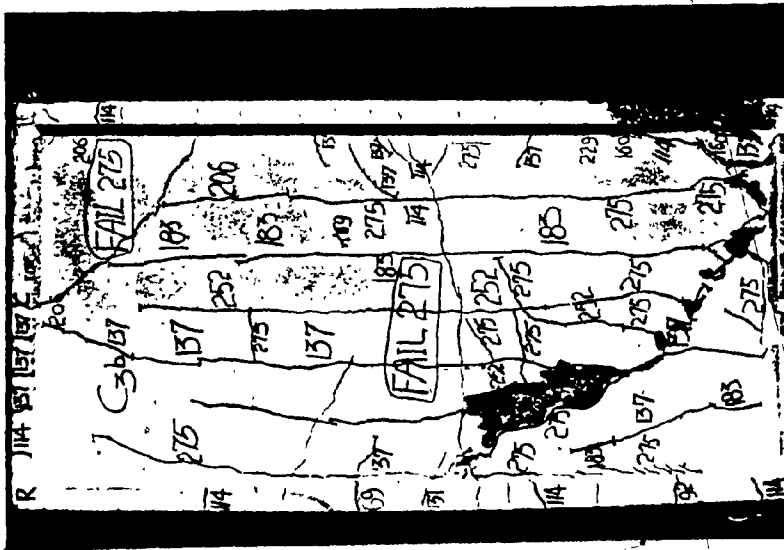


Figure A7
Back View of Panel C3 (At Failure)



Figure A9
Overall View of the Tested Panels (At Failure)

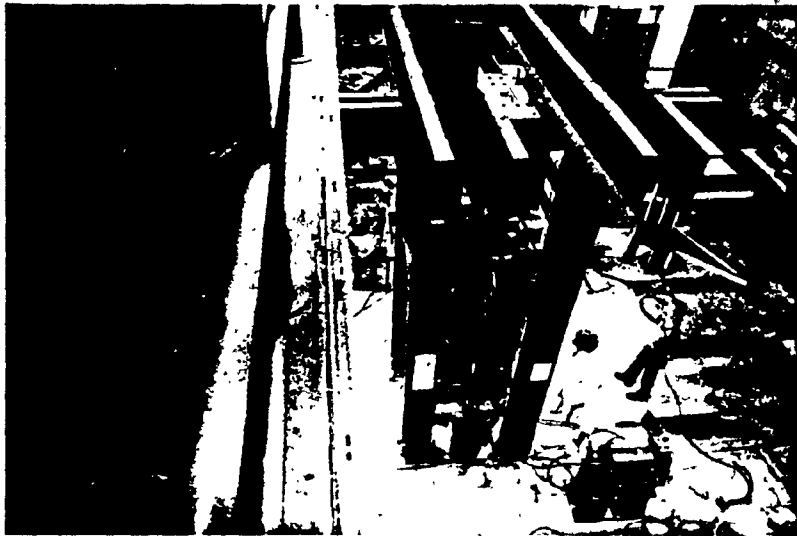


Figure A10
Overall View of the Testing Frame